Local transformation leading to an efficient Fourier modal method for perfectly conducting gratings

Simon Félix,[1,*] Agnès Maurel,[2] and Jean-François Mercier[3]

[1]*LAUM, CNRS, Université du Maine, avenue Olivier Messiaen, 72085 Le Mans, France*
[2]*Institut Langevin, CNRS, ESPCI ParisTech, 1 rue Jussieu, 75005 Paris, France*
[3]*Poems, CNRS, ENSTA ParisTech, INRIA, 828 boulevard des Maréchaux, 91762 Palaiseau, France*
**Corresponding author: simon.felix@univ-lemans.fr*

Received June 27, 2014; accepted August 13, 2014;
posted August 20, 2014 (Doc. ID 214623); published September 19, 2014

We present an efficient Fourier modal method for wave scattering by perfectly conducting gratings (in the two polarizations). The method uses a geometrical transformation, similar to the one used in the C-method, that transforms the grating surface into a flat surface, thus avoiding to question the Rayleigh hypothesis; also, the transformation only affects a bounded inner region that naturally matches the outer region; this allows applying a simple criterion to select the ingoing and outgoing waves. The method is shown to satisfy reciprocity and energy conservation, and it has an exponential rate of convergence for regular groove shapes. Besides, it is shown that the size of the inner region, where the solution is computed, can be reduced to the groove depth, that is, to the minimal computation domain.

OCIS codes: (050.0050) Diffraction and gratings; (000.4430) Numerical approximation and analysis; (050.1950) Diffraction gratings; (050.2770) Gratings; (260.2110) Electromagnetic optics.
http://dx.doi.org/10.1364/JOSAA.31.002249

1. INTRODUCTION

Numerical methods to simulate the diffraction of waves by gratings have experienced successive improvements over the last decades. For penetrable gratings, the Fourier modal method, or rigorous coupled-wave analysis, has reached a high degree of accuracy and it is the most popular method being used today for modeling diffraction by penetrable gratings [1–8]. The case of impenetrable gratings, with Dirichlet boundary conditions (b.c.s) for transverse electric waves or Neumann b.c.s for transverse magnetic waves, is subject to more controversy. This is partially because many studies are concerned with the inspection of the Rayleigh hypothesis ([9–13] and [14], Chap. 10). In his original work [15], Rayleigh made the assumption that the scattered field inside the grooves can be expanded onto a series of waves moving away from the grating surface. This is *a priori* valid for shallow gratings, and much effort has been dedicated to inspect the range of validity of this hypothesis. In parallel to these studies, a few works have proposed to use geometrical transformations that do not rely on the Rayleigh hypothesis. The so-called C-method has been proposed by Chandezon and co-workers in a series of papers [16–20]; it uses a translation coordinate system that transforms the grating surface into a plane surface. Further studies have then presented a comparison of this method with classical ones, such as the Rayleigh–Fourier method [21–23]. However, because the C-method uses a geometrical transformation that affects the whole space, applying the radiation condition may appear to be difficult, since the selection of outgoing waves is not straightforward and requires eigensolutions to be determined. More recently, Shcherbakov and Tishchenko [24] introduced a geometrical transformation in some bounded region containing the grating, so that the new coordinates continuously match the natural Cartesian coordinates. This is in our opinion a key point that allows natural matching to the outer region where the radiation condition has to be accounted for. Note that this concept of matching the outer region is of prime importance in geometrical (or optical) transformations as used for cloaking or, say more generally, wave control [25,26]. In this paper, we use the same idea of a "local" geometrical transformation for impenetrable gratings. Otherwise, our proposed numerical scheme is similar to the Fourier modal method and can be implemented straightforwardly.

A noticeable improvement in the method presented concerns convergence, which is often not reported quantitatively in the literature. The convergence of a numerical method for any problem is limited by the regularity of the field computed. For penetrable gratings, the wave field has a discontinuous gradient, which limits the convergence of the method to a power law $N^{-3/2}$, N being the truncation order of the Fourier, or modal, series [27]. If the limit of a perfectly conducting grating is considered, the error in the Fourier method is known to increase, but the convergence in terms of power law is the same; the shortcomings of the method, if any, may be due to a large error for low truncation or to the fact that the error enters in its power law decay for high truncation; we have not seen in the literature a representation of the error able to answer this question. In the present paper, these limiting cases are directly treated as impenetrable gratings and this modifies the convergence drastically. Indeed, our geometrical transformation leads to a modified wave equation in a continuously varying medium, with space-dependent coefficients having the same regularity as the groove profile. For smooth profiles (described by a function of class C^∞), this produces a

convergence with exponential rate, much better than the usual power laws.

The key steps of the method presented are (1) the geometrical transformation leading to a modified wave equation expressed in a bounded region of space; (2) the introduction of an auxiliary field to get a system of coupled, first-order differential equations, with simple b.c.s; and (3) the modal expansions of the two wave fields leading to a usual system of evolution equations for the modal components. Steps 2 and 3 are similar to the (E,H) formulation in the Fourier modal method. Finally, the modal components expressed in the virtual space do not question the Rayleigh hypothesis.

The paper is organized as follows: in Section 2, the modal formulation, Eq. (17), is derived. Section 3 is concerned with the numerical resolution. In the present paper, we use the impedance matrix, or the admittance matrix (Section 3.A), and implement a Magnus scheme (Section 3.B). However, the Fourier modal method, based on the scattering matrix, would be as efficient to solve our system of coupled equations, Eq. (17). In addition to illustrative examples, where the method is validated by comparison with a finite-element code, in Section 4 we inspect the convergence of the method and the influence of the size of the transformed region, where the calculation is performed. Concluding remarks are presented in Section 5.

2. MODAL FORMULATION IN THE TRANSFORMED SPACE

We consider a perfectly conducting grating whose profile is described in the real space (X,Y) by a periodic function $Y=f(X)$, with period d (Fig. 1). The grating is illuminated from vacuum $[Y>f(X)]$ by a monochromatic plane wave with wavenumber k and incidence angle θ. The harmonic time dependence with angular frequency ω is $e^{-i\omega t}$, and it will be omitted in the following. The wave is polarized, with either the electric field parallel to the grooves, $\mathbf{E}=E(X,Y)\mathbf{e}_Z$, referred to as transverse electric (TE) waves, or the magnetic field parallel to the grooves, $\mathbf{H}=H(X,Y)\mathbf{e}_Z$, referred to as transverse magnetic (TM) waves. For TE waves, a Dirichlet b.c. is imposed at the surface of the perfectly conducting grating, whereas for TM waves, a Neumann b.c. applies.

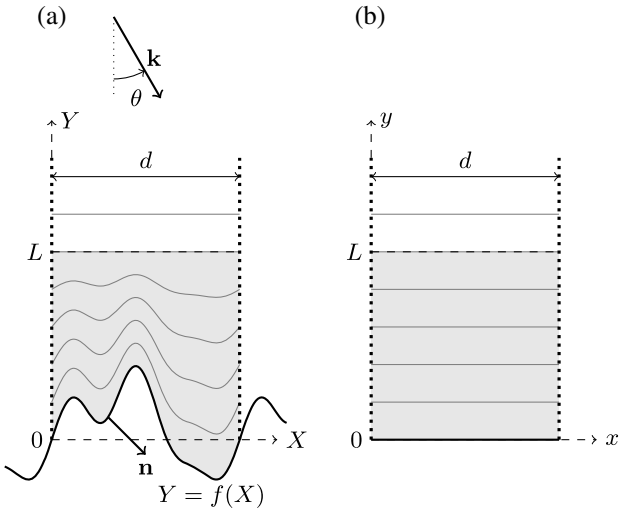

Fig. 1. (a) Grating in real space with (X,Y) coordinates, being d-periodic along X, illuminated by a wave (TE or TM) with wavenumber k at incidence θ. The isolines of the y-values resulting from the geometrical transformation [Eq. (4)] are shown, with $y=0$ on the grating surface and $y=L=Y$ being invariant. (b) Resulting virtual space in (x,y) coordinates.

A. Geometrical Transformation

The wave field u, being either the electric field $u=E$ for TE waves or the magnetic field $u=H$ for TM waves, satisfies the Helmholtz equation

$$(\Delta+k^2)u=0, \tag{1}$$

with periodic b.c.s (respectively, essential and natural b.c.s)

$$u(d,Y)=e^{i\beta d}u(0,Y), \tag{2a}$$

$$\partial_X u(d,Y)=e^{i\beta d}\partial_X u(0,Y), \tag{2b}$$

and $\beta\equiv k\sin\theta$. On the grating surface $Y=f(X)$,

$$\begin{cases} u=0 & \text{(Dirichlet b.c., in TE)},\\ \mathbf{n}\cdot\nabla u=\partial_Y u-f'\partial_X u=0 & \text{(Neumann b.c., in TM)}. \end{cases} \tag{3}$$

Next, we define a new coordinate system (x,y) (transformed space) deduced from (X,Y) in the real space:

$$x\equiv X,\qquad y\equiv\begin{cases} L\frac{Y-f(X)}{L-f(X)}, & f(X)\le Y\le L\\ Y, & Y>L. \end{cases} \tag{4}$$

The transformation is local, in the sense that for $Y>L$, the virtual and real spaces coincide; this is of importance when the radiation condition will be taken into account. In practice, the numerical solution is computed in the transformed region $(0\le y\le L)$ that corresponds to the region $(f(X)\le Y\le L)$ in the real space; we present below the calculations in that region.

B. Modified Wave Equation and Boundary Conditions

According to the theory of transformation media, mapping of the coordinates $(X,Y)\to(x,y)$ results in a change of the parameters appearing in the wave equation, Eq. (1). Denoting J as the Jacobian tensor of the geometrical transformation, we obtain in the (x,y) virtual space

$$\nabla\cdot\left(\frac{{}^t\mathsf{J}\mathsf{J}}{\det\mathsf{J}}\nabla u\right)+\frac{k^2}{\det\mathsf{J}}u=0, \tag{5}$$

where the information in the variable change (or metric information) translates, for TE waves, into a new permeability tensor ${}^t\mathsf{J}\mathsf{J}/\det\mathsf{J}$ and a new permittivity $1/\det\mathsf{J}$ (respectively, a new tensor of permittivity and a new permeability for TM waves) that vary in space. Owing to Eq. (4), we get

$$\mathsf{J}=\begin{pmatrix} 1 & -a/b\\ 0 & 1/b \end{pmatrix}, \tag{6}$$

where

$$a(x,y)\equiv f'(x)\frac{L-y}{L},\qquad b(x)\equiv\frac{L-f(x)}{L}, \tag{7}$$

and with $\det \mathsf{J} = 1/b$,

$$\frac{{}^t\mathsf{J}\mathsf{J}}{\det \mathsf{J}} = \begin{pmatrix} b & -a \\ -a & (1+a^2)/b \end{pmatrix}. \tag{8}$$

Here, we have denoted $u(x,y) = u(X,Y)$ and $f(x) = f(X)$ in the virtual space to avoid multiple notations. The transformed wave equation, Eq. (5) reads as

$$\partial_x(b\partial_x u - a\partial_y u) + \partial_y(-a\partial_x u + (1+a^2)/b\partial_y u) + k^2 b u = 0. \tag{9}$$

Next, rather than dealing with this second-order equation on u, it is preferable to use coupled first-order evolution equations along y. To do that, we use an auxiliary wave field $v(x,y)$ defined as

$$v \equiv -a\partial_x u + \frac{(1+a^2)}{b}\partial_y u, \tag{10}$$

which is basically the quantity that is derived with respect to y in Eq. (9). We get the desired coupled-wave equations on (u,v):

$$\begin{cases} \partial_y u &= \frac{ab}{1+a^2}\partial_x u + \frac{b}{1+a^2} v, \\ \partial_y v &= -bk^2 u - \partial_x\left(\frac{b}{1+a^2}\partial_x u\right) + \partial_x\left(\frac{ab}{1+a^2} v\right), \end{cases} \tag{11}$$

with the b.c.s being translated into

$$u(d,y) = e^{i\beta d} u(0,y), \tag{12a}$$

$$\left[\partial_x u - \frac{a}{b}\partial_y u\right]_{x=d} = e^{i\beta d}\left[\partial_x u - \frac{a}{b}\partial_y u\right]_{x=0}, \tag{12b}$$

which means u and $\partial_x u$ are pseudoperiodic; then, at the grating surface $y = 0$, the b.c.s for either TE or TM polarization take the simple form

$$\begin{cases} u(x,0) = 0 & \text{(for Dirichlet b.c.)}, \\ v(x,0) = 0 & \text{(for Neumann b.c.)}. \end{cases} \tag{13}$$

C. Coupled Modal Wave Equations

The fields $u(x,y)$ and $v(x,y)$ are now expanded as

$$\begin{cases} u(x,y) = \sum_{n=-\infty}^{+\infty} u_n(y)\varphi_n(x), \\ v(x,y) = \sum_{n=-\infty}^{+\infty} v_n(y)\varphi_n(x), \end{cases} \tag{14}$$

and here, the $\varphi_n(x)$ are chosen as

$$\varphi_n(x) = \frac{1}{\sqrt{d}} e^{i(\beta + 2n\pi/d)x}, \tag{15}$$

to satisfy the pseudoperiodic b.c.s. Note that the choice of φ_n as cosine or sine functions can be used straightforwardly to treat the case of waves propagating in Neumann or Dirichlet waveguides [27]. The common properties of the bases are the orthogonality relations

$$(\varphi_m, \varphi_n) = \delta_{mn} \quad \text{and} \quad (\varphi'_m, \varphi'_n) = \gamma_n^2 \delta_{mn}, \tag{16}$$

with $(f,g) = \int_0^d \mathrm{d}x \bar{f} g$ the scalar product. In the present case, we have $\gamma_n = \beta + 2n\pi/d$.

Let us stress again that in our transformation, as in [16,17,24], the grating surface coincides with $y = 0$, which means the expansion, Eq. (14) does not question the Rayleigh hypothesis. This is because the modal components $u_n(y)$ are not equal to the modal components $u_n(Y)$ that would have been defined by expanding $u(X,Y)$ in the real space.

The projection of Eq. (11) on the basis $\{\varphi_n\}$ leads to a set of first-order coupled equations governing the modal components $\mathbf{u} \equiv (u_n)$ and $\mathbf{v} \equiv (v_n)$:

$$\frac{\partial}{\partial y}\begin{pmatrix} \mathbf{u} \\ \mathbf{v} \end{pmatrix} = \begin{pmatrix} \mathsf{A}(y) & \mathsf{B}(y) \\ -k^2\mathsf{B}(L) + \mathsf{C}(y) & -\mathsf{A}^*(y) \end{pmatrix}\begin{pmatrix} \mathbf{u} \\ \mathbf{v} \end{pmatrix}, \tag{17}$$

with

$$\mathsf{A}_{mn} = \int_0^d dx \frac{ab}{1+a^2}\bar{\varphi}_m \varphi'_n, \tag{18a}$$

$$\mathsf{B}_{mn} = \int_0^d dx \frac{b}{1+a^2}\bar{\varphi}_m \varphi_n, \tag{18b}$$

$$\mathsf{C}_{mn} = \int_0^d dx \frac{b}{1+a^2}\bar{\varphi}'_m \varphi'_n, \tag{18c}$$

and A^* the conjugate transpose of A. Note that using the Bloch–Floquet modes (15), C is simply $\mathsf{C} = -\Gamma\mathsf{B}\Gamma$, with Γ the diagonal matrix given by $\Gamma_m = i\gamma_m$.

3. NUMERICAL SCHEME

Several methods exist to solve the system of two coupled linear differential equations, Eq. (17). More often, it is solved using scattering matrix or reflection matrix methods that avoid the use of a transfer matrix, known to produce numerical instabilities. Here, we present an alternative way based on the use of the impedance Z (or admittance Y) matrix [27,28].

A. Admittance/Impedance Matrices

The impedance matrix Z links the two vectors $\mathbf{u}$ and $\mathbf{v}$ through $\mathbf{u} = \mathsf{Z}\mathbf{v}$. Z is known to satisfy a Riccati equation, from Eq. (17),

$$\mathsf{Z}' = \mathsf{B} + \mathsf{A}\mathsf{Z} + \mathsf{Z}\mathsf{A}^* + \mathsf{Z}[k^2\mathsf{B}(L) - \mathsf{C}]\mathsf{Z}, \tag{19}$$

that can be solved given an initial condition. For TE waves, $u = E$ vanishes at $y = 0$, leading to the initial condition $\mathsf{Z}(0) = 0$.

Since, for TM waves, the b.c. at $y = 0$ is $v = 0$ [Eq. (13)], we rather use the admittance matrix Y that is the inverse of the impedance matrix $\mathbf{v} = \mathsf{Y}\mathbf{u}$. Thus, it can be integrated with the initial condition $\mathsf{Y}(0) = 0$. In the following section, we present the Magnus scheme used to integrate the impedance/admittance matrix and, if needed, to compute the wave field.

B. Magnus Scheme

Basically, the coupled-wave equations for the modal components [Eq. (17)] are written formally as

$$\frac{\partial}{\partial y}\begin{pmatrix} \mathbf{u} \\ \mathbf{v} \end{pmatrix} = \mathsf{M}(y)\begin{pmatrix} \mathbf{u} \\ \mathbf{v} \end{pmatrix}, \tag{20}$$

and are solved using a Magnus scheme,

$$\begin{pmatrix}\mathbf{u}\\ \mathbf{v}\end{pmatrix}(y) = \exp[-\mathsf{M}(y+dy/2)dy]\begin{pmatrix}\mathbf{u}\\ \mathbf{v}\end{pmatrix}(y+dy), \tag{21}$$

where the step size dy depends on the truncation order N of the infinite series, that is, using the expansions

$$u(x,y) = \sum_{n=-N}^{N} u_n(y)\varphi_n(x) \tag{22}$$

(same for v). Indeed, to capture the variations of the most evanescent mode considered in the truncation, typically, $k_N = \sqrt{k^2-\gamma_N^2} = i\alpha_N$, we fix $dy = 1/\alpha_N$. We define the matrix F:

$$\mathsf{F}(y+dy/2) \equiv \exp[-\mathsf{M}(y+dy/2)dy] = \begin{pmatrix}\mathsf{F}_{11} & \mathsf{F}_{12}\\ \mathsf{F}_{21} & \mathsf{F}_{22}\end{pmatrix}, \tag{23}$$

where each F_{ij} is a $(2N+1)\times(2N+1)$ matrix.

The problem is solved numerically in two steps, only the first of which is necessary to get the scattering properties. In the first step, only Z (or Y) is calculated. To do that, we translate on Z the relations $\mathbf{u}(y) = \mathsf{F}_{11}\mathbf{u}(y+dy) + \mathsf{F}_{12}\mathbf{v}(y+dy)$ and $\mathbf{v}(y) = \mathsf{F}_{21}\mathbf{u}(y+dy) + \mathsf{F}_{22}\mathbf{v}(y+dy)$, where F is evaluated at $(y+dy/2)$ to get

$$\mathsf{Z}(y+dy) = [\mathsf{Z}(y)\mathsf{F}_{21} - \mathsf{F}_{11}]^{-1}[\mathsf{F}_{12} - \mathsf{Z}(y)\mathsf{F}_{22}] \tag{24}$$

and the integration is performed from $\mathsf{Z}(0) = 0$ to $\mathsf{Z}(L)$.

Similarly, for TM waves, the integration is performed from $\mathsf{Y}(0) = 0$ to $\mathsf{Y}(L)$ using

$$\mathsf{Y}(y+dy) = [\mathsf{F}_{22} - \mathsf{Y}(y)\mathsf{F}_{12}]^{-1}[\mathsf{Y}(y)\mathsf{F}_{11} - \mathsf{F}_{21}]. \tag{25}$$

Accounting for the source term is easy when $\mathsf{Z}(L)$ or $\mathsf{Y}(L)$ is known. This is because, as in [13], the coordinate transform concerns only the bounded region $0 \le y \le L$. Thus, at the boundaries $y = L$ (and $\mathsf{Y} = y \ge L$), the waves correspond to the physical, incident and reflected, waves in the real space; this has to be opposed to the C-method, where the physical incident and reflected waves have to be determined in the virtual space (being unbounded). We have, thus, for $y \ge L$,

$$u(x,y) = e^{-ik\cos\theta y}\varphi_0(x) + \sum_{n=-N}^{N} R_n e^{ik_n(y-L)}\varphi_n(x) \tag{26}$$

and $v = \partial_y u$, leading to

$$\begin{cases} u_n(L) = e^{-ik\cos\theta L}\delta_{n0} + R_n,\\ v_n(L) = -ik\cos\theta e^{-ik\cos\theta L}\delta_{n0} + ik_n R_n, \end{cases} \tag{27}$$

from which the reflection coefficients R_n (calculated at $y = L$) can be deduced by inversion of the relations

$$[ik_n\delta_{mn} - \mathsf{Y}_{mn}(L)]R_n = [ik\cos\theta\delta_{m0} + \mathsf{Y}_{m0}(L)]e^{-ik\cos\theta L} \tag{28}$$

or

$$[ik_n\mathsf{Z}_{mn}(L) - \delta_{mn}]R_n = [ik\cos\theta\mathsf{Z}_{m0}(L) + \delta_{m0}]e^{-ik\cos\theta L}. \tag{29}$$

If the wave field is looked for, then it is sufficient to store the impedance matrix or admittance matrix at each y. If so, then the wave field is calculated starting from the initial values $u_n(L)$ or $v_n(L)$ in Eq. (27); then, coming back to Eq. (21), we use $\mathbf{u}(y) = \mathsf{F}_{11}\mathbf{u}(y+dy) + \mathsf{F}_{12}\mathbf{v}(y+dy)$ and $\mathbf{v}(y) = \mathsf{F}_{21}\mathbf{u}(y+dy) + \mathsf{F}_{22}\mathbf{v}(y+dy)$ to get, from $y = L$ to $y = 0$,

$$\mathbf{u}(y) = [\mathsf{F}_{11} + \mathsf{F}_{12}\mathsf{Y}(y+dy)]\mathbf{u}(y+dy) \tag{30}$$

or

$$\mathbf{v}(y) = [\mathsf{F}_{21}\mathsf{Z}(y+dy) + \mathsf{F}_{22}]\mathbf{v}(y+dy). \tag{31}$$

In the latter case, the wave field $u(y)$ is deduced from $v(y)$ using $u(y) = Z(y)v(y)$.

C. Reciprocity and Energy Conservation

In this section, we check that our formulation, Eq. (17) satisfies the reciprocity relation and it conserves the energy. Reciprocity links two solutions u_A and u_B of the problem, namely,

$$\nabla\cdot[u_A\nabla u_B - u_B\nabla u_A] = 0, \tag{32}$$

which translates, on our modal components, to

$$\partial_y[{}^t\mathbf{u}_A\bar{\mathbf{v}}_B - {}^t\bar{\mathbf{u}}_B\mathbf{v}_A] = 0, \tag{33}$$

where we considered that the u solution implies the $\bar{u}$ solution (time reversal invariance of the Helmholtz equation). The energy conservation simply follows by choosing $\mathbf{u}_A = \mathbf{u}_B = \mathbf{u}$, leading to the conservation of the Poynting vector $\partial_y\Pi = 0$, with

$$\Pi(y) \propto \mathrm{Im}[{}^t\bar{\mathbf{u}}\mathbf{v}]. \tag{34}$$

Since B and C are self-adjoint matrices, it follows directly that the reciprocity, Eq. (33) and the energy conservation $\partial_y\Pi = 0$ are satisfied. In practice, the energy conservation is checked by inspecting the value of $|e-1|$,

$$e \equiv \sum_n |R_n|^2\frac{k_n}{k\cos\theta}, \tag{35}$$

being the normalized reflected energy [with the notations in Eq. (26), and where the sum is performed with the propagating modes only]; in all the results presented, the energy conservation has been found to be satisfied within $|e-1| \sim 10^{-11}$–10^{-15}.

4. RESULTS

Before a more quantitative inspection of the numerical method, we report in Fig. 2 examples of fields computed for complex shapes of the grating surface; in each case, the profiles are generated by summing sine and cosine functions (d-periodic; see figure caption); either TM polarization (Neumann b.c.) or TE polarization (Dirichlet b.c.) has been considered in the examples, and the nondimensional frequency kd has been chosen such that the wavelength is of the same order as the grooves in Figs. 2(a) and 2(b), much larger [rough surface type in Fig. 2(c)], and much smaller [Fig. 2(d)]. Note, in Fig. 2(b), the typical cat-eye pattern observed at the cut-off frequency and corresponding to the Rayleigh–Wood anomaly (see, e.g., [14], chapter 8). The modal

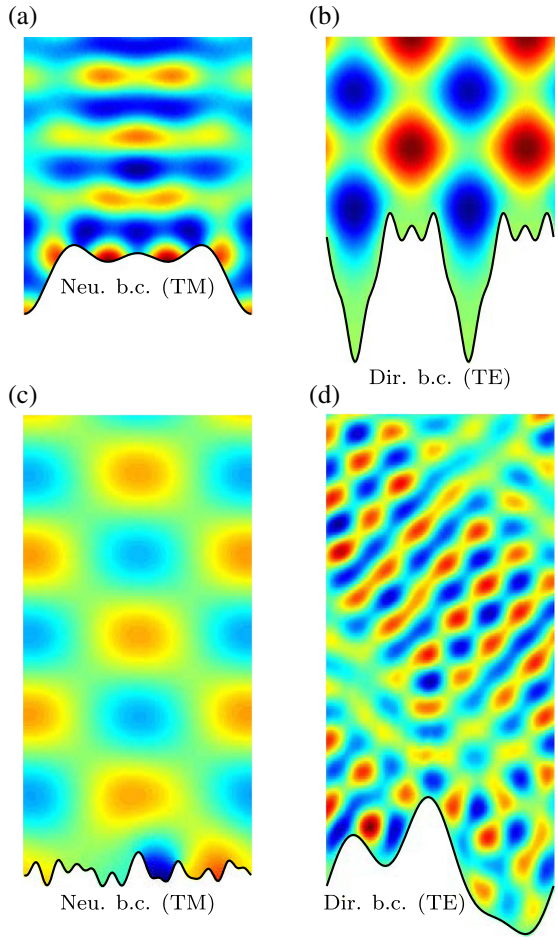

Fig. 2. Real part of the wave field $u(x,y)$ for grating shapes $f(x) = \sum_p a_p \cos(2p\pi x/d) + b_p \sin(2p\pi x/d)$. (a) $\{a_p/d\}_{p=1,3} = [-0.08, -0.08, -0.06]$ (zero b_p) and $kd = 7.5\pi$, $\theta = 0$ (TM). (b) $a_2 = 0.25d$, $b_1 = -0.5d$, $b_5 = -0.1d$ (zero otherwise), and $kd = 2\pi$, $\theta = 0$ (TE). (c) For both a_p and b_p: 15 values chosen randomly, $kd = 3.5\pi$, $\theta = -\pi/5$ (TM). (d) $\{a_p/d\}_{p=1,3} = [-0.13, 0.10, -0.04]$, $\{b_p/d\} = [0.19, 0.03, 0.07]$, and $kd = 10.5\pi$, $\theta = \pi/4$ (TE).

calculation has been validated by comparison with a finite-element code [29]; for the profile in Fig. 2(a), the difference between the computed fields is 9% with $N = 10$ and 1% with $N = 13$; for the profile in Fig. 2(b), at a lower frequency, the difference between the computed fields is 10% with $N = 7$ and 1.5% with $N = 10$.

In the following sections, we inspect the convergence of the method and the influence of the length L of the transformed region in the case of a sine shape.

A. Convergence

The results of the convergence of the method have been obtained for a simple sine shape $f(x) = 0.5d(1 - \cos 2\pi x/d)$, and $kd = 7.5\pi$, $\theta = \pi/4$. The modal components u_n are shown to decrease exponentially with n [Fig. 3(a)]. This fast rate of decay is expected for infinitely differentiable $f(x)$ shapes. Indeed, this results in all the coefficients in Eq. (9) being infinitely differentiable; hence, u and v behave the same. Also, the φ_n functions are adapted, which means here that they are pseudoperiodic (and all their derivatives). This behavior of the modal components produces an exponential convergence of the wave field as well. This is illustrated in Fig. 3(b), where we report the behavior of $\varepsilon_N \equiv \|u - u^{ex}\|/\|u^{ex}\|$, with u the solution truncated at order N [Eq. (22)], and where u^{ex} refers to an exact solution (in practice, calculated for a large N-value). Note that the case of penetrable gratings would produce a convergence with a power law decay [27], because of the discontinuities in the contrasts between the two media; obviously, any power law is worse than the exponential decay.

B. Influence of the Size L of the Transformed Region

Figure 4 illustrates the fact that the field calculated does not depend on L, even in the limiting case where $L = \max(f)$, that is, when only the grooves are resolved.

More quantitatively, we report in Fig. 5 the behavior of the reflection coefficient R_0 of the mode 0 for varying L-values; also, the conservation of the energy given by $|e - 1|$ [Eq. (35)] is shown. For both TE and TM polarizations, small variations of $|R_0|$ are visible for L in the range $[\max(f), 4\max(f)]$, whose amplitude decreases when increasing N. This fact, together with the fact that the energy is conserved even for $L = \max(f)$, shows that the calculation domain can be reduced to its minimum size (the groove thickness).

C. Remark on Profiles with Discontinuous Derivatives

Obviously there are no restrictions to considering grating profiles with one of their derivatives being discontinuous; this is illustrated in Fig. 6 for a profile with a discontinuous first derivative and a profile with a discontinuous second derivative. In these cases, the convergence is degraded, from exponential decay to a power law decay ($\sim N^{-1}$ and $\sim N^{-3}$ for the given examples), as observed in other problems [27,30]. Generally, we expect a power law convergence $N^{-\alpha}$, with α related to the regularity of the profile function (e.g., to the

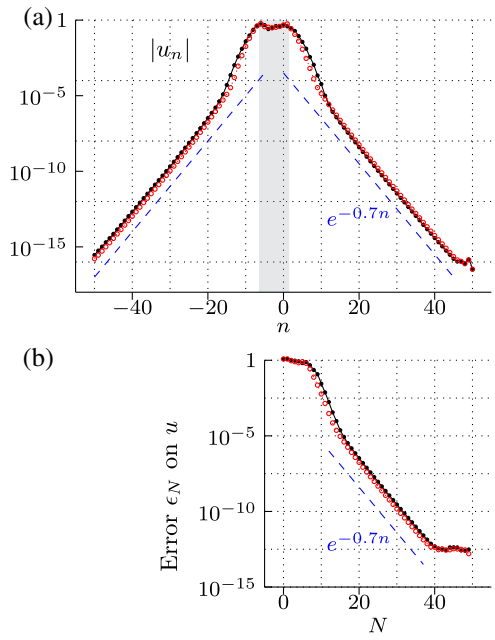

Fig. 3. (a) Rate of decay of the modal components $|u_n|$ (averaged over y); the gray strip indicates the n-values corresponding to propagating modes. (b) Convergence of the wave field $|u|$ [averaged over x and y for $L = 2\max(f)$]. In both figures, for TM polarization (dotted lines with open symbols) and TE polarization (solid lines with closed symbols).

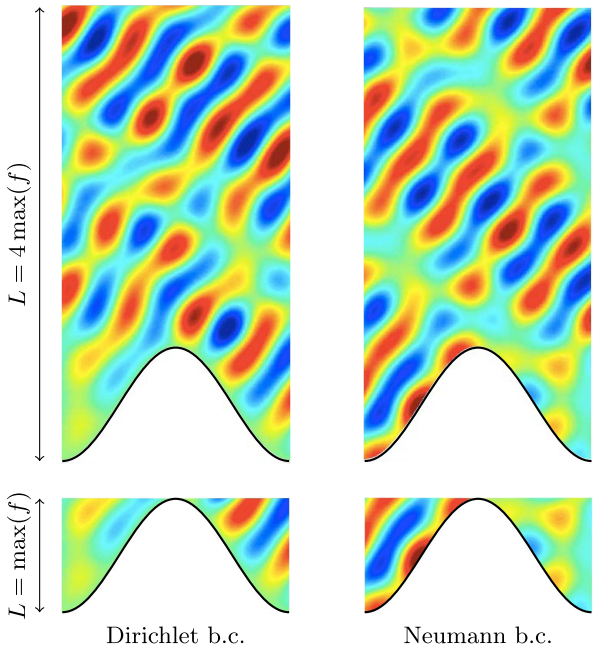

Fig. 4. Examples of fields computed for a sine shape $f(x) = a_0(1 - \cos 2\pi x/d)$, $a_0 = 0.25d$, $kd = 7.5\pi$, and $\theta = \pi/4$ [$\max(f) = 0.5d$]. At the bottom, for $L = \max(f)$ and on top, for $L = 4\max(f)$.

order of the first discontinuous derivative). While increasing the regularity of the function, the exponential decay is recovered progressively.

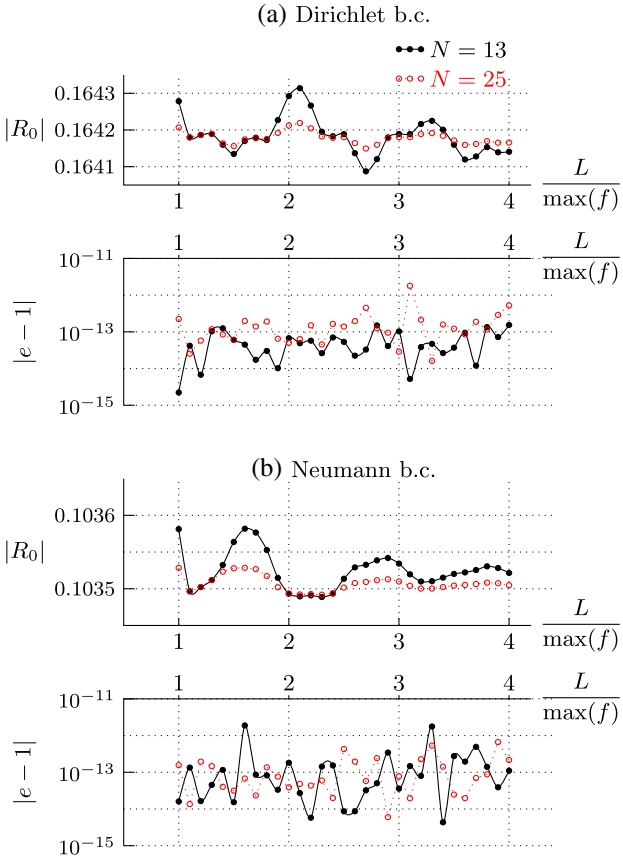

Fig. 5. Reflection coefficient R_0 as a function of L for the configurations in Fig. 4 and $N = 13, 25$; energy conservation measured by $|e - 1|$ [see Eq. (35)] as a function of L.

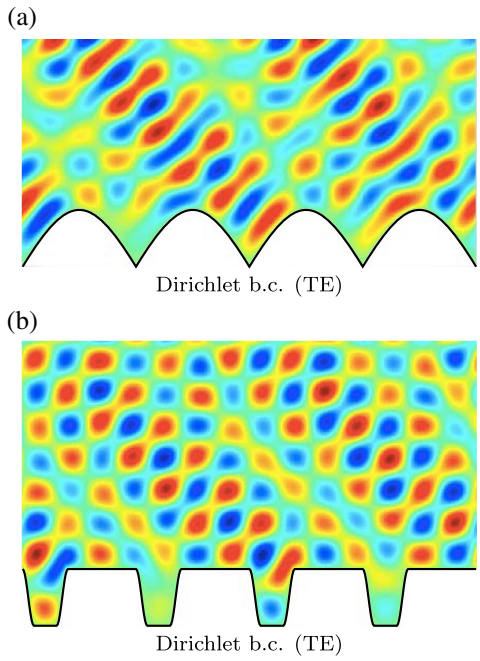

Fig. 6. Examples of wave fields for grating profiles having (a) a discontinuous first derivative and (b) a discontinuous second derivative.

However, the case of a profile with, locally, an infinite first derivative [e.g., a discontinuous function $f(X)$] cannot be treated, although the multimodal equation, Eq. (17) remains workable numerically. The Jacobian (6) becomes infinite if f' is infinite, preventing a proper bijective coordinate change to be performed.

5. CONCLUSION

An efficient Fourier method is presented, for scattering by perfectly conducting gratings, either in TE or TM wave polarization. We use the idea of a geometrical transformation, introduced earlier in the C-method [16,17], that transforms the grating surface into a plane surface, thus avoiding to question the Rayleigh hypothesis. Besides, as introduced recently in [24] for penetrable gratings, our transformation is local and matches the outer region continuously, which makes the radiation conditions easy to account for. The resulting system of coupled equations, Eq. (17), describes the wave propagation in the inner (rectangular) transformed region, and the space-dependent coefficients encapsulate the complexity of the groove shape. Note that a Magnus scheme has been used to solve this system, but it could be solved equivalently using the Fourier modal method. The method has been validated by comparison with a finite-element code, and it has been shown that it presents the following advantages: (1) it ensures reciprocity and energy conservation; (2) the inner region, where the calculations are performed, can be reduced to its minimum size, that is, the thickness of the grooves; and (3) the convergence of the method is exponential, which is the best convergence expected. Finally, a significant advantage of our formalism (not addressed in the present paper) is that it is well suited for perturbative calculations, as done in Ref. [31].

Note, finally, that the present method can be implemented straightforwardly in the case of waves propagating in waveguides, in 2D and 3D, and this will be done elsewhere.

ACKNOWLEDGMENTS

The authors thank G. Favraud and V. Pagneux for valuable discussions. This work is supported by the Agence Nationale de la Recherche through grant ANR ProCoMedia, project ANR-10-INTB-0914. A.M. acknowledges the financial support of the LABEX WIFI (Laboratory of Excellence within the French Program "Investments for the Future") under references ANR-10-LABX-24 and ANR-10-IDEX-0001-02 PSL*.

REFERENCES

1. M. G. Moharam and T. K. Gaylord, "Rigorous coupled-wave analysis of planar-grating diffraction," J. Opt. Soc. Am. **71**, 811–818 (1981).
2. M. G. Moharam and T. K. Gaylord, "Rigorous coupled-wave analysis of grating diffraction—E-mode polarization and losses," J. Opt. Soc. Am. **73**, 451–455 (1983).
3. P. Lalanne and G. M. Morris, "Highly improved convergence of the coupled-wave method for TM polarization," J. Opt. Soc. Am. A **13**, 779–784 (1996).
4. L. Li, "Use of Fourier series in the analysis of discontinuous periodic structures," J. Opt. Soc. Am. A **13**, 1870–1876 (1996).
5. E. Popov and M. Nevière, "Grating theory: new equations in Fourier space leading to fast converging results for TM polarization," J. Opt. Soc. Am. A **17**, 1773–1784 (2000).
6. E. Popov and M. Nevière, "Maxwell equations in Fourier space: fast-converging formulation for diffraction by arbitrary shaped, periodic, anisotropic media," J. Opt. Soc. Am. A **18**, 2886–2894 (2001).
7. G. Granet and B. Guizal, "Analysis of strip gratings using a parametric modal method by Fourier expansions," Opt. Commun. **255**, 1–11 (2005).
8. B. Guizal, H. Yala, and D. Felbacq, "Reformulation of the eigenvalue problem in the Fourier modal method with spatial adaptive resolution," Opt. Lett. **34**, 2790–2792 (2009).
9. R. F. Millar, "The Rayleigh hypothesis and a related least squares solution to scattering problems for periodic surfaces and other scatterers," Radio Sci. **8**, 785–796 (1973).
10. P. M. Van den Berg and J. T. Fokkema, "The Rayleigh hypothesis in the theory of reflection by a grating," J. Opt. Soc. Am. **69**, 27–31 (1979).
11. T. Watanabe, Y. Choyal, K. Minami, and V. L. Granatstein, "Range of validity of the Rayleigh hypothesis," Phys. Rev. E **69**, 056606 (2004).
12. J. Wauer and T. Rother, "Considerations to Rayleigh's hypothesis," Opt. Commun. **282**, 339–350 (2009).
13. A. V. Tishchenko, "Numerical demonstration of the validity of the Rayleigh hypothesis," Opt. Express **17**, 17102–17117 (2009).
14. E. G. Loewen and E. Popov, *Diffraction Gratings and Applications* (CRC Press, 1997).
15. L. Rayleigh, "On the dynamical theory of gratings," Proc. R. Soc. London, Ser. A **79**, 399–416 (1907).
16. J. Chandezon, G. Raoult, and D. Maystre, "A new theoretical method for diffraction gratings and its numerical application," J. Opt. **11**, 235–241 (1980).
17. J. Chandezon, M. T. Dupuis, G. Cornet, and D. Maystre, "Multicoated gratings: a differential formalism applicable in the entire optical region," J. Opt. Soc. Am. **72**, 839–846 (1982).
18. L. Li, G. Granet, J. P. Plumey, and J. Chandezon, "Some topics in extending the C method to multilayer gratings of different profiles," Pure Appl. Opt. **5**, 141–156 (1996).
19. L. Li, J. Chandezon, G. Granet, and J. P. Plumey, "Rigorous and efficient grating-analysis method made easy for optical engineers," Appl. Opt. **38**, 304–313 (1999).
20. A. Y. Poyedinchuk, Y. A. Tuchkin, N. P. Yashina, J. Chandezon, and G. Granet, "C-method: several aspects of spectral theory of gratings," Prog. Electromagn. Res. **59**, 113–149 (2006).
21. E. Popov and L. Mashev, "Convergence of Rayleigh–Fourier method and rigorous differential method for relief diffraction gratings," J. Mod. Opt. **33**, 593–605 (1986).
22. T. Vallius, "Comparing the Fourier modal method with the C method: analysis of conducting multilevel gratings in TM polarization," J. Opt. Soc. Am. A **19**, 1555–1562 (2002).
23. K. Edee, J. P. Plumey, and J. Chandezon, "On the Rayleigh–Fourier method and the Chandezon method: comparative study," Opt. Commun. **286**, 34–41 (2013).
24. A. A. Shcherbakov and A. V. Tishchenko, "Efficient curvilinear coordinate method for grating diffraction simulation," Opt. Express **21**, 25236–25247 (2013).
25. J. B. Pendry, D. Schurig, and D. R. Smith, "Controlling electromagnetic fields," Science **312**, 1780–1782 (2006).
26. N. I. Landy and W. J. Padilla, "Guiding light with conformal transformations," Opt. Express **17**, 14872–14879 (2009).
27. A. Maurel, J.-F. Mercier, and S. Félix, "Wave propagation through penetrable scatterers in a waveguide and though a penetrable grating," J. Acoust. Soc. Am. **135**, 165–174 (2014).
28. V. Pagneux, "Multimodal admittance method in waveguides and singularity behavior at high frequencies," J. Comput. Appl. Math. **234**, 1834–1841 (2010).
29. D. Martin, "Melina Version 2.5 (2011)," http://anum-maths.univ-rennes1.fr/melina/danielmartin/melina/ (accessed: 3 September 2014).
30. A. Maurel, J.-F. Mercier, and V. Pagneux, "Improved multimodal admittance method in varying cross section waveguides," Proc. R. Soc. London, Ser. A **470**, 20130448 (2014).
31. A. Maurel, S. Félix, J.-F. Mercier, A. Ourir, and Z. E. Djeffal, "Wood's anomalies for arrays of dielectric scatterers," J. Eur. Opt. Soc. **9**, 14001 (2014).